Desalination and Water Treatment
www.deswater.com

doi: 10.5004/dwt.2017.20677

77 (2017) 135–141
May

The performance of the spiral wound and flat sheet forward osmosis elements with thin film composite membrane

Jongmin Jeon[a], Jaehak Jung[a], Joon Young Choi[b], Suhan Kim[a,*]

[a]*Department of Civil Engineering, Pukyong National University, 45 Yongso-ro, Nam-gu, Busan 608-737, Korea, Tel. +82-51-629-6065, Fax: +82-51-629-6063; email: suhankim@pknu.ac.kr (S. Kim)*
[b]*Hyorim Industries, Inc., Institute of Technology, 1161-73, Jisan-dong, Suseong-gu, Daegu, Korea*

Received 6 October 2016; Accepted 16 December 2016

ABSTRACT

The two different types (flat sheet and spiral wound) of commercial forward osmosis (FO) elements with thin film composite membrane were tested to understand the effects of concentrations and cross-flow velocities of feed solution (FS) and draw solution (DS) on the performance of the element. An FO element tester was customized for reliable measurements of water flux and reverse solute flux during operation time when the concentration difference between DS and FS was decreased. The test results reveal that: (1) the water flux and reverse solute flux increases at higher concentration differences between FS and DS, (2) the higher crossflow velocity increases water flux by decreasing the effects of external concentration polarization, (3) the pressure differential between the inlet and the outlet of the FO element increases at higher crossflow velocities, which may limit the crossflow velocity in a full-scale FO design, (4) the flat sheet element exhibits up to 25 LMH of water flux comparable to the water flux (30–35 LMH) in the coupon tests, and (5) the spiral wound FO element shows a peculiar flux pattern in which the increasing rate of water flux becomes retarded when water flux exceeds a critical value maybe because the DS channel in the FO membrane envelop may not allow a flow rate higher than a critical value due to complexity in the DS flow direction.

Keywords: Forward osmosis; Element; Flat sheet; Spiral wound; Thin film composite

1. Introduction

Forward osmosis (FO) process, as a desalination method, has been studied intensively in the last decade [1–4]. FO uses osmotic pressure for filtration instead of using mechanical pressure like reverse osmosis (RO) does. Due to its low pressure characteristics, FO is more advantageous than RO in terms of energy consumption and low fouling [4–9]. Recently, FO applications cover not only seawater desalination but also wider areas such as wastewater treatment, food processing, microalgae harvesting, and so forth [10–14].

Most of the published papers about the FO process focused on the water and salt transfer mechanisms through the FO membrane. The internal and external concentration polarizations (ECP) are key parameters determining the performance of the FO membrane [2,4,15–20]. However, these results were based upon the lab-scale experiments using small-sized coupons of FO membranes. In the real-scale application, FO membrane elements (or modules) should be used instead of the coupons. Since the FO element has much wider membrane areas than the coupon, the filtration behaviors should be different according to the spatial positions in the element. The feed solution (FS) becomes concentrated and the draw solution (DS) is diluted as they flow inside the FO element. Thus, the coupon-based FO membrane characteristics cannot directly interpret the performance of the FO elements.

The modeling approaches for the FO elements make it possible to account for the spatial variations of the filtration characteristics [13,14,21]. By modeling the concentrated FS and the diluted DS with the consideration of the channel shape inside the FO element, the overall filtration performance

* Corresponding author.

(i.e., the average water and solute flux) of the element can be predicted. However, most of these model-based studies were not applicable to a full-scale FO process design by themselves because some of them are not verified experimentally and some of them need the model parameter estimation procedure using the actual FO element tests [21,22]. Thus, the FO element tests are essential to design a full-scale process and it is very important to experimentally analyze the characteristics of FO elements.

There are several studies dealing with the FO element tests [10,21–24]. Attarde et al. [21,22] tested a commercial spiral wound element (HTI, Albany, USA) and used the experimental results to estimate the modeling parameter. Lotfi et al. [10] tested a self-developed thin film composite hollow fiber element using fertilizer as DS. Shibuya et al. [24] carried out the FO element test using a commercial cellulose triacetate hollow fiber module (Toyobo, Japan) and compared the experimental results with the theoretical prediction. Kim et al. [23] tested a commercial spiral wound element (HTI, Albany, USA) with two different spacers. Most of the FO element tests mentioned above reported flux data <10 LMH with 1 M (or higher concentration) of DS concentration (NaCl), which does not help the full-scale FO application be promising.

Recently, two commercial FO elements using thin film composite membrane with high flux were developed. One is spiral wound type by Toray Chemical Korea Inc. (Gumi, Korea) and the other is flat sheet type by Porifera Inc (Hayward, CA, USA). In this work, the two FO elements were tested and the factors affecting the performance of the elements such as FS and DS concentrations, crossflow velocity were investigated. To the authors' best knowledge, this paper is the first one to publish the performance of the two FO elements.

2. Methods

2.1. FO elements

In this work, two FO elements were tested and named "A" and "B" for convenience. A schematic diagram of "A" element is shown in Fig. 1(a) [24]. FS and DS channels are separated by a flat membrane sheet. Each DS channel is separated by impermeable layer. The area of thin film composite FO membrane is 7 m^2 and the dimensions of FS and DS channels are listed in Table 1. Pressure at any port in the "A" element must not exceed 1 bar and transmembrane pressure should be <0.2 bar. The flow directions of FS and DS are perpendicular to each other.

"B" element is a spiral wound type as shown in Fig. 1(b). FS flows into the FS channel (like the feed channel in a spiral wound RO element) and DS flows into the central tube first and then is introduced to the DS channel by several holes. Each membrane sheet is separated by the FS spacer and the sheets with the spacers are glued together as shown in Fig. 1(b) [23]. The area of thin film composite FO membrane is 15.3 m^2 and the dimensions of FS and DS channels are shown in Table 1.

2.2. FO element test

In order to test the two FO elements, an FO element tester was setup as shown in Fig. 2. The two elements, "A" and "B" are installed in the tester and the element desired for testing can be selected by valve control. FS and DS flow into the tested FO element and re-circulated to their own tanks, which results in concentrating FS and diluting DS during the test. The volume of each tank is 400 L. FS flow rate (Q_f), concentrate flow rate (Q_c), feed concentration (C_f), concentrate concentration (C_c), DS flow rate (Q_d), and DS concentration (C_d) can be monitored in real time. Pressure gauges are located in front of each FO elements. Input flow rates to the element (Q_f and Q_d) are controlled by valves. The diluted DS flow rate (Q_{dd}) and concentration (C_{dd}) can be calculated based on the mass balance inside the element using:

$$Q_{dd} = Q_d + (Q_f - Q_c) \quad (1)$$

$$C_{dd} = \frac{(Q_d C_d + Q_f C_f - Q_c C_c)}{Q_{dd}} \quad (2)$$

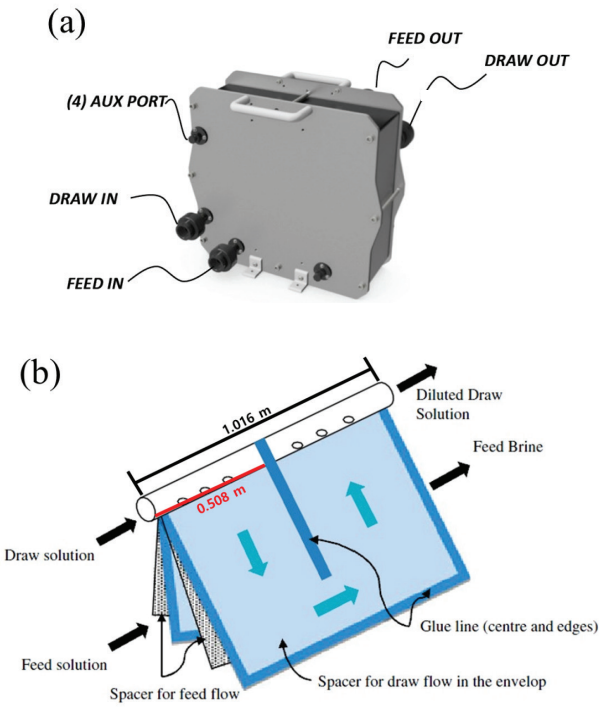

Fig. 1. Schematic diagram of elements: (a) "A" element and (b) "B" element [23,25].

Table 1
Dimensions of FS and DS channels for the FO elements [25]

FO element	"A"		"B"	
	FS	DS	FS	DS
Thickness (cm)	0.071	0.038	0.081	0.162
Width (cm)	34.45	30.80	125.5	50.8
Void fraction (%)	60	95	60[a]	95[a]
The number of channels	34	66	12	12
Cross-sectional area (cm^2)	49.98	73.57	73.19	93.81

[a]Assumed values.

The average water flux of FO element (J_w) is calculated by:

$$J_w = \frac{Q_f - Q_c}{A_m} \quad (3)$$

where A_m is total membrane area of the element. Reverse solute flux (J_s) is calculated based on the mass balance inside the FS channel using:

$$J_s = \frac{(Q_c C_c - Q_f C_f)}{A_m} \quad (4)$$

Sodium chloride (NaCl) from industrial refined salt (OCI Co. Ltd., China) was used as draw solute and pure water was used as FS at the start of the FO element test. The pure water was produced by a bench-scale RO system with tap water as RO feed and a 4-inch seawater RO membrane (RE4040-SHN, Toray Chemical Korea). Sodium bisulfite was added to the tap water to remove free chlorine and protect the RO membrane [26].

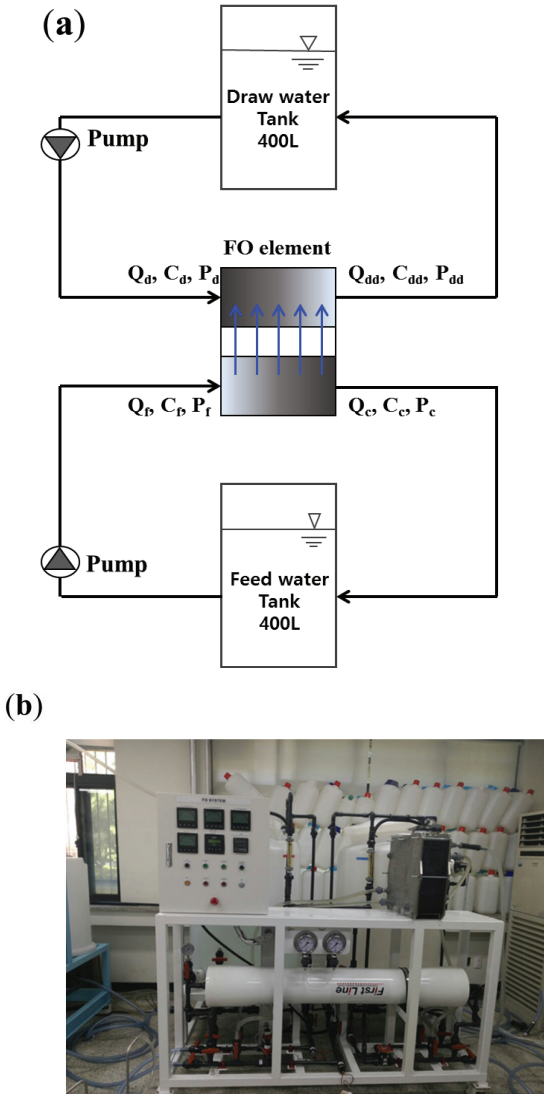

Fig. 2. Experimental setup for FO element: (a) flow diagram and (b) picture of the FO element tester.

At the start for every test, DS and FS concentrations are set to 1 M as NaCl and 0 M, respectively. During the test DS is diluted and FS becomes concentrated, and thus the concentration difference between DS and FS decreases with time, which makes it possible to investigate the effect of FS and DS concentration on the performance of FO elements. In order to see the effect of FS and DS crossflow velocities, various combinations of FS and DS flow rates were tested.

3. Results and discussion

3.1. Basic analysis of FO element tests

In a general FO element test using FO element tester as shown in Fig. 2, DS is diluted and FS is concentrated during operation, which causes the decline of water and solute flux with time. Fig. 3 shows the results of a duplicate set of FO element tests using "A" element. The diluted DS and concentrated FS during the operation come from two reasons: (1) DS is diluted and FS is concentrated while passing through their own channels, and (2) the diluted DS and concentrated FS are returned to their own tanks after passing through the FO element. The first reason accounts for the difference between C_d (or C_f) and C_{dd} (or C_c) as shown in Figs. 3(a) and (b), and the second reason induces the decline of C_d (Fig. 3(a)) and the increase of C_f (Fig. 3(b)). The sudden increase of FS concentration in Fig. 3(b) comes from sodium chloride spiked into the feed tank. As shown in Fig. 3(c), water flux decreases with time because FS is concentrated and DS is diluted (i.e., the difference between DS and FS concentrations decreases with operation time). The highest flux observed is 25 LMH at 1 M (as NaCl) of DS concentration, which is comparable with the flux (30–35 LMH) in the coupon test [25].

Fig. 3(d) shows reverse solute flux calculated using Eq. (4) during the test. Interestingly, the reverse solute flux data obtained after spiking NaCl into the feed tank are scattered in disorder. This is because the fluctuations of conductivity measurements exceed the actual reverse solute transfer rates when feedwater conductivity is higher than a critical value (e.g., ~200 μS/cm in this test). Below the critical feedwater conductivity (observed within 50 min of operation time in this test), the reverse solute flux couples with water flux and decreases with time because the difference between DS and FS concentrations decreases with operation time. This result provides one important tip when analyzing reverse solute flux: FS concentration should be near zero (or less than a critical value) to obtain reliable reverse solute flux data.

3.2. Effect of concentration and crossflow velocity

Since the difference between DS and FS concentrations plays a major role to determine the water and solute flux of an FO element, it should be better if these flux data are expressed as a function of $C_d - C_f$. It is clearly seen that the water flux increases at larger $C_d - C_f$ values as shown in Fig. 4(a). The water flux increases at the faster FS and DS crossflow velocities because of two possible reasons [13]: (1) the increased ECP resulted from the increased crossflow velocity leads to the increase in the actual osmotic pressure

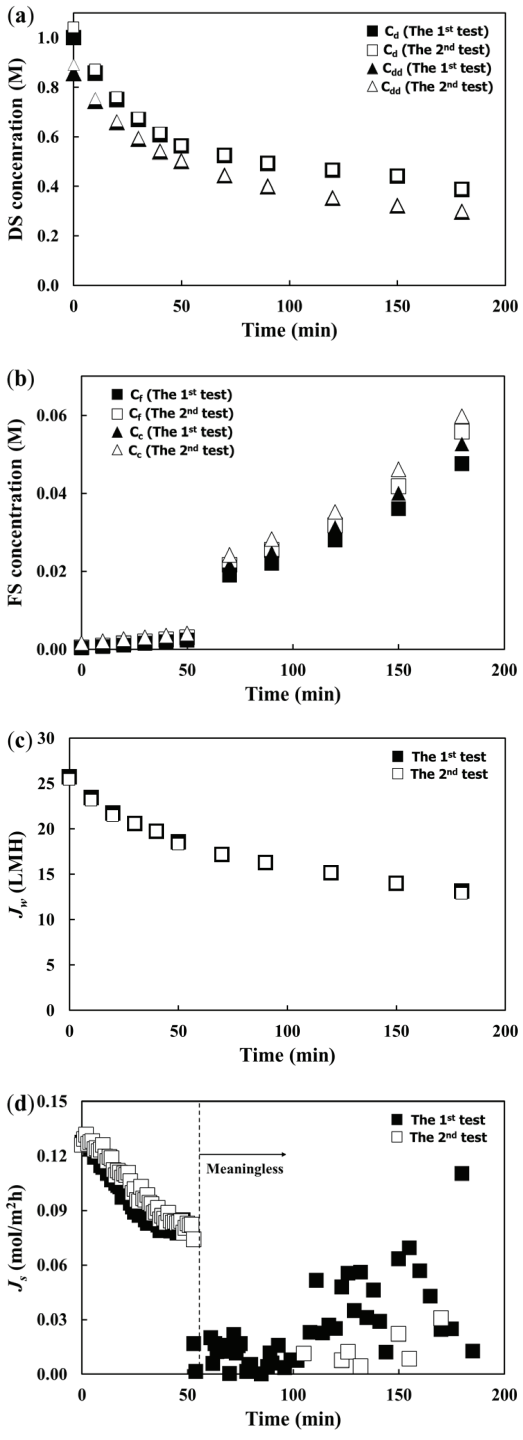

Fig. 3. A full set of FO element test results (FS crossflow velocity = 6.01 cm/s, DS crossflow velocity = 4.08 cm/s, FO element = "A", and temperature = 23°C): (a) DS concentration, (b) FS concentration, (c) water flux, and (d) reverse solute flux.

difference between DS and FS, and (2) the degrees of concentrated FS and diluted DS become smaller at higher crossflow rates of FS and DS, respectively (e.g., $C_d - C_{dd}$ decreases at higher DS crossflow rates, and $C_d - C_f$ differs from the actual difference between DS and FS). In order to minimize the effect of the second reason, it would be better if water flux is expressed as a function of the difference between the actual DS and FS concentrations in the FO element like:

$$\text{DS} - \text{FS concentration (actual)} = \frac{C_d + C_{dd}}{2} - \frac{C_f + C_c}{2} \quad (5)$$

Therefore, the flux difference according to crossflow velocity in Fig. 4(b) should come from the ECP effect only. In Fig. 4(a), the average increase in water flux is 2.8 LMH as FS and DS crossflow velocities increase by 1.8 times (i.e., from the lowest to the highest values in Fig. 5(a)). The average increase in water flux in Fig. 3(b) is 2.5 LMH, which is regarded as pure effect of ECP and it covers almost 90% (≅ 2.5/2.8) of total effects.

In order to achieve the same water flux, the more concentrated DS is needed when DS and FS crossflow rates become smaller. By analyzing data in Fig. 4(a), 0.15 M (on average) of additional sodium chloride is needed to maintain the same water flux when FS and DS crossflow velocities are decreased by 1.8 times (i.e., from the highest to the lowest values in Fig. 4(a)).

Fig. 4(c) shows the reverse solute flux as a function of $C_d - C_f$. In the case of the highest DS and FS crossflow velocities (5.21 and 7.67 cm/s, respectively), we were not able to access the reliable reverse solute flux data because the starting conductivity of FS exceeded 270 μS/cm at the test, which is higher value than the feedwater conductivity in the "meaningless" zone (<200 μS/cm) in other two cases. Again, it can be said that it is very important to control the staring feedwater conductivity to near zero in order to obtain reverse solute flux data. As shown in the two reliable data groups (i.e., 4.08 cm/s (DS) – 6.01 cm/s (FS) and 2.94 cm/s (DS) – 4.34 cm/s (FS)) in Fig. 4(c), it is found that the reverse solute flux increases at higher $C_d - C_f$ and crossflow velocity values like the water flux patterns as shown in Fig. 4(a) or (b).

Although higher crossflow velocity is beneficial to the performance of FO elements, it should be noticed that the pressure differential (ΔP, the pressure difference between inlet and outlet of the FO element) increases at higher crossflow velocities as shown in Fig. 4(d). Especially for the case of "A" element, the applied pressure is limited to 1 bar at any entry of the element so that special caution is needed.

3.3. Comparison between two FO elements

Fig. 5(a) shows the comparison between "A" and "B" elements during the element test with 1.0 M NaCl solution as DS and pure water as FS. Both elements show the increase in water flux at larger $C_d - C_f$ values. However, the increasing rate of water flux in the case of "B" element is evidently smaller than that in the case of "A" element. In the lower $C_d - C_f$ values, "B" element shows better performance than "A" element in terms of water flux. For example, water flux (14.9 LMH) of "B" element at 0.40 M of $C_d - C_f$ value is much higher than that (8.57 LMH) of "A" element at the same condition and the flux difference between the two elements becomes smaller at higher $C_d - C_f$ values. Finally, water flux (18.82 LMH) of "B" element is outrun by that (20.57 LMH) of "A" element at 0.98 M of $C_d - C_f$ value. The flux pattern of "B" element is quite strange when the flux data at 0.4 and 0.98 M of $C_d - C_f$ values are compared (i.e., 14.9 LMH (0.40M) vs. 18.82

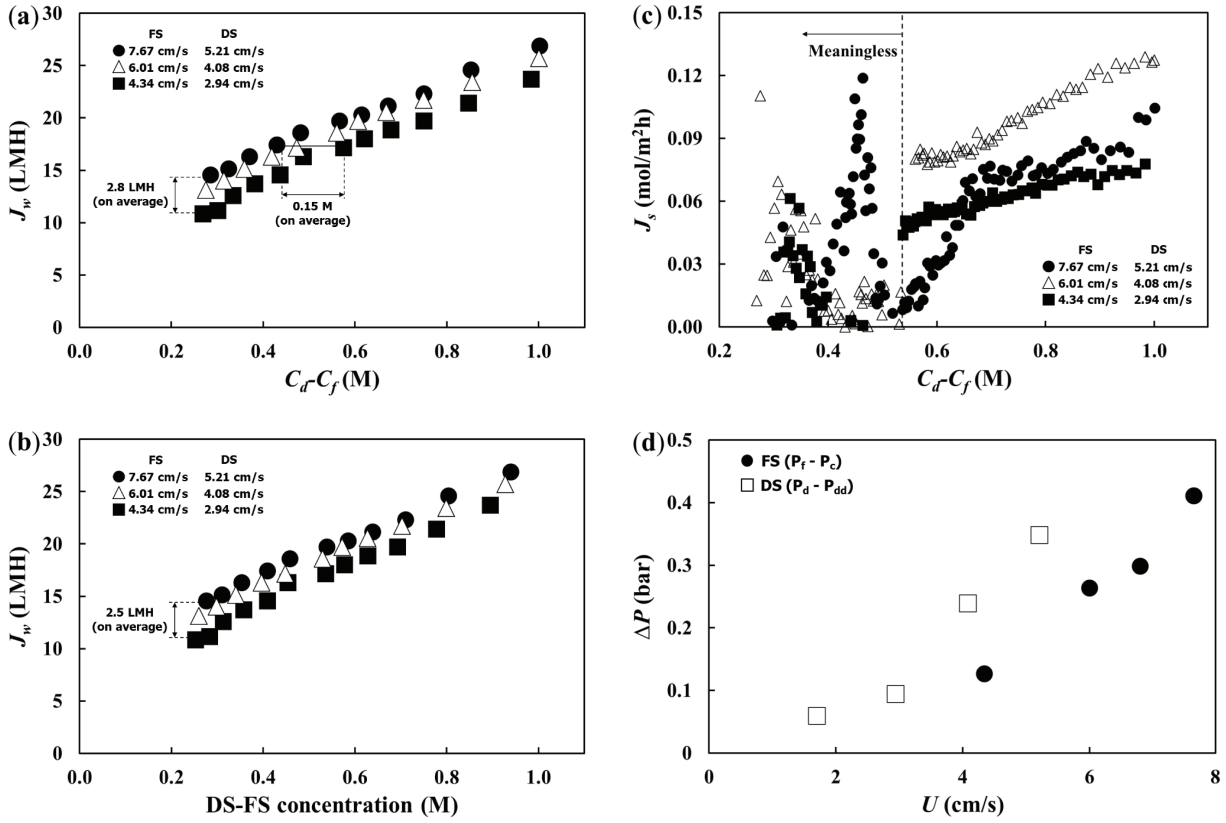

Fig. 4. Effect of FS and DS crossflow velocity on the performance of "A" element at 23°C: (a) J_w vs. $C_d - C_f$, (b) J_w vs. DS–FS concentration (actual), (c) J_s vs. $C_d - C_f$, and (d) ΔP vs. crossflow velocity (U).

LMH (0.98M)). Water flux increases from 0 to 14.9 LMH as $C_d - C_f$ value increases from 0 to 0.40 M, but it increases by additional 3.72 LMH as $C_d - C_f$ value increases by 0.58 M (i.e., from 0.40 to 0.98 M). Experimental errors may be suspected. However, as shown in the duplicate testing results (Fig. 5(b)), the flux patterns of "A" and "B" elements in the second test are almost the same as those in the first test (Fig. 5(a)). In addition, the reverse solute flux data in Fig. 5(c) mean that there is no defect of FO membrane sheets in both "A" and "B" elements during the test.

In the region where $C_d - C_f$ value is smaller than 0.40 M in Fig. 5(b), the flux increasing pattern of "B" element is similar to that of "A" element. This result implies that something weird happens in "B" element when $C_d - C_f$ value is higher than 0.40 M (or, water flux is higher than 14 LMH). One probable hypothesis for this weird performance of "B" element is that the DS channel in the FO membrane envelope may not allow a DS flow rate higher than a critical value due to the complexity in the DS flow direction as shown in Fig. 1(b). More tests should be carried out to clearly explain the peculiar flux pattern observed in "B" element.

4. Conclusions

This paper provides experimental results using two different types of commercial FO elements (flat sheet and spiral wound types) with thin film composite membrane. Effects of concentrations and crossflow velocities of FS and DS were investigated and a brief comparison between the two FO elements was carried out. The key findings are summarized as follows:

- The water flux and reverse solute flux increase at higher concentration differences between FS and DS.
- The reverse solute flux cannot be obtained when feed conductivity is high enough to produce fluctuation in measurement.
- The water flux and reverse solute flux increase at higher crossflow velocities mostly due to the smaller effects of ECP. The effect of concentrated FS and diluted DS during operation affect much less than ECP. In the case of the flat sheet module tested at 23°C, water flux increases by 2.8 LMH if FS and DS crossflow velocities are increased by 1.8 times, and 0.15 M of additional DS (NaCl) is needed to maintain the same water flux if FS and DS crossflow velocities are decreased by 1.8 times.
- The pressure differential between the inlet and the outlet of the FO element increases at higher crossflow velocities, which may limit the crossflow velocity in a full-scale FO design.
- The flat sheet element exhibits up to 25 LMH of water flux with 1.0 M as NaCl of DS concentration, which is comparable with the water flux (30–35 LMH) in the coupon tests.
- The spiral wound FO element exhibits a peculiar flux pattern in which the increasing rate of water flux becomes

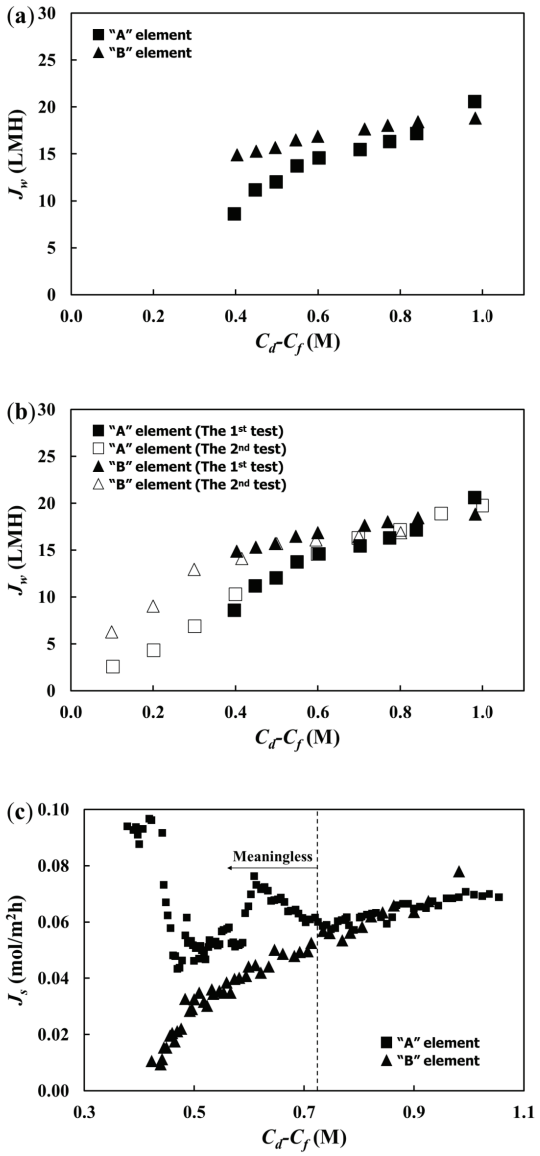

Fig. 5. Comparison between "A" and "B" elements (FS crossflow velocity = 6.7 cm/s, DS crossflow velocity = 1.8 cm/s, and temperature = 18°C): (a) J_w in the first test, (b) J_w in duplicate testing, and (c) J_s in the first test.

retarded when water flux exceeds a critical value (e.g., ~14 LMH in the test presented in Fig. 5). The DS channel in the FO membrane envelop may not allow a flow rate higher than a critical value due to complexity in the DS flow direction.

This work focused on the methodology to analyze a typical FO element test and provided some interesting findings discussed above. On the basis of the accomplishment of this work, a model-based approach to quantitatively characterize FO elements should be carried out in future works in order to design a full-scale FO system.

Acknowledgments

This research was supported by a grant (16IFIP-B088091-04) from Industrial Facilities & Infrastructure Research Program funded by Ministry of Land, Infrastructure and Transport of Korean government.

References

[1] T.Y. Cath, A.E. Childress, M. Elimelech, Forward osmosis: principles, applications, and recent developments, J. Membr. Sci., 281 (2006) 70–87.
[2] J.R. McCutcheon, M. Elimelech, Modeling water flux in forward osmosis: implications for improved membrane design, AIChE J., 53 (2007) 1736–1744.
[3] W.C.L. Lay, T.H. Chong, C.Y. Tang, A.G. Fane, J. Zhang, Y. Liu, Fouling propensity of forward osmosis: investigation of the slower flux decline phenomenon, Water Sci. Technol., 61 (2010) 927–936.
[4] J.R. McCutcheon, M. Elimelech, Influence of concentrative and dilutive internal concentration polarization on flux behavior in forward osmosis, J. Membr. Sci., 284 (2006) 237–247.
[5] A. Achilli, T.Y. Cath, E.A. Marchand, A.E. Childress, The forward osmosis membrane bioreactor: a low fouling alternative to MBR processes, Desalination, 239 (2009) 10–21.
[6] M. Elimelech, W.A. Phillip, The future of seawater desalination: energy, technology, and the environment, Science, 333 (2011) 712–717.
[7] B. Mi, M. Elimelech, Organic fouling of forward osmosis membranes: fouling reversibility and cleaning without chemical reagents, J. Membr. Sci., 348 (2010) 337–345.
[8] C.R. Martinetti, A.E. Childress, T.Y. Cath, High recovery of concentrated RO brines using forward osmosis and membrane distillation, J. Membr. Sci., 331 (2009) 31–39.
[9] J. Jeon, B. Park, Y Yoon, S. Kim, An optimal design of forward osmosis and reverse osmosis hybrid process for seawater desalination, Desal. Wat. Treat., 57 (2016) 26612–26620.
[10] F. Lotfi, S. Phuntsho, T. Majeed, K. Kim, D.S. Han, A. Abdel-Wahab, H.K. Shon, Thin film composite hollow fibre forward osmosis membrane module desalination of brackish groundwater for fertigation, Desalination, 364 (2015) 108–118.
[11] S. Zhao, L. Zou, C.Y. Tang, D. Mulcahy, Recent developments in forward osmosis: opportunities and challenges, J. Membr. Sci., 396 (2012) 1–21.
[12] S. Kim, S. Paudel, G.T. Seo, Forward osmosis membrane filtration for microalgae harvesting cultivated in sewage effluent, Environ. Eng. Res., 20 (2015) 99–104.
[13] S. Kim, Scale-up of osmotic membrane bioreactors by modelling salt accumulation and draw solution dilution using hollow-fiber membrane characteristics and operation conditions, Bioresour. Technol., 165 (2014) 88–95.
[14] S.H. Park, B. Park, H.K. Shon, S. Kim, Modeling full-scale osmotic membrane bioreactor systems with high sludge retention and low salt concentration factor for wastewater reclamation, Bioresour. Technol., 190 (2015) 508–515.
[15] R. Wang, L. Shi, C.Y.Y. Tang, S.R. Chou, C. Qiu, A.G. Fane, Characterization of novel forward osmosis hollow fiber membranes, J. Membr. Sci., 355 (2010) 158–167.
[16] G.T. Gray, J.R. McCutcheon, M. Elimelech, Internal concentration polarization in forward osmosis: role of membrane orientation, Desalination, 197 (2006) 1–8.
[17] W. Li, Y. Gao, C.Y. Tang, Network modeling for studying the effect of support structure on internal concentration polarization during forward osmosis: model development and theoretical analysis with FEM, J. Membr. Sci., 379 (2011) 307–321.
[18] C.Y. Tang, Q. She, W.C.L. Lay, R. Wang, A.G. Fane, Coupled effects of internal concentration polarization and fouling on flux behavior of forward osmosis membranes during humic acid filtration, J. Membr. Sci., 354 (2010) 123–133.

[19] J. Lee, S. Kim, Predicting power density of pressure retarded osmosis (PRO) membranes using a new characterization method based on a single PRO test, Desalination, 389 (2016) 224–234.
[20] J. Lee, J.Y. Choi, J-S. Choi, K.H. Chu, Y. Yoon, S. Kim, A statistics-based forward osmosis membrane characterization method without pressurized reverse osmosis experiment, Desalination, 403 (2017) 36–45.
[21] D. Attarde, M. Jain, S. K. Gupta, Modeling of a forward osmosis and a pressure-retarded osmosis spiral wound module using the Spiegler-Kedem model and experimental validation, Sep. Purif. Technol., 164 (2016) 182–197.
[22] D. Attarde, M. Jain, K. Chaudhary, S.K. Gupta, Osmotically driven membrane processes by using a spiral wound module – modeling, experimentation and numerical parameter estimation, Desalination, 361 (2015) 81–94.
[23] J.E. Kim, S. Phuntsho, F. Lotfi, H.K. Shon, Investigation of pilot-scale 8040 FO membrane module under different operating conditions for brackish water desalination, Desal. Wat. Treat., 53 (2015) 2782–2791.
[24] M. Shibuya, M. Yasukawa, S. Goda, H. Sakurai, T. Takahashi, M. Higa, H. Matsuyama, Experimental and theoretical study of a forward osmosis hollow fiber membrane module with a cross-wound configuration, J. Membr. Sci., 504 (2016) 10–19.
[25] Porifera Inc., PFO-100 User Manual, Version 2.1. (2015). Available at: http://www.porifera.com
[26] M. Kim, M. Kim, B. Park, S. Kim, Changes in characteristics of polyamide reverse osmosis membrane due to chlorine attack, Desal. Wat. Treat., 54 (2015) 4–5.